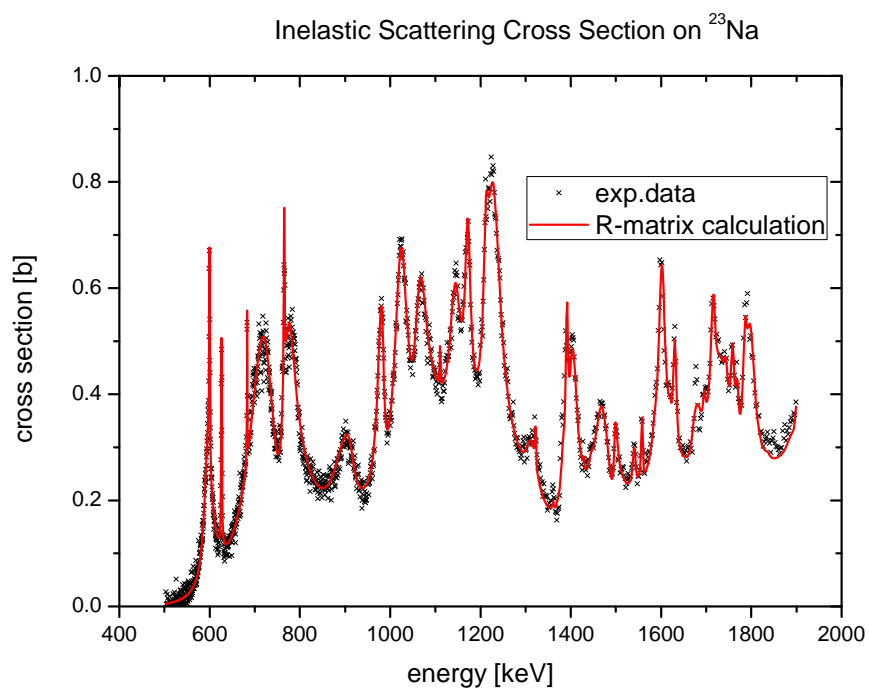


## JRC Scientific and Technical Reports

# R-matrix analysis of the total and inelastic scattering cross section of $^{23}\text{Na}$

S. Kopecky and A.J.M. Plompen



EUR 25067 EN - 2011

The mission of the JRC-IRMM is to promote a common and reliable European measurement system in support of EU policies.

European Commission  
Joint Research Centre  
Institute for Reference Materials and Measurements

**Contact information**

Address: S. Kopecky, Retieseweg 111, 2440 Geel, Belgium  
E-mail: [Stefan.Kopecky@ec.europa.eu](mailto:Stefan.Kopecky@ec.europa.eu)  
Tel.: +32-14-571 479  
Fax: +32-14 574 862

<http://irmm.jrc.ec.europa.eu/>  
<http://www.jrc.ec.europa.eu/>

**Legal Notice**

Neither the European Commission nor any person acting on behalf of the Commission is responsible for the use which might be made of this publication.

***Europe Direct is a service to help you find answers  
to your questions about the European Union***

**Freephone number (\*):**

**00 800 6 7 8 9 10 11**

(\* ) Certain mobile telephone operators do not allow access to 00 800 numbers or these calls may be billed.

A great deal of additional information on the European Union is available on the Internet. It can be accessed through the Europa server <http://europa.eu/>

JRC 67884

EUR 25067 EN  
ISBN 978-92-79-22214-6  
ISSN 1831-9424  
doi:10.2787/55514

Luxembourg: Publications Office of the European Union, 2011

© European Union, 2011

Reproduction is authorised provided the source is acknowledged

*Printed in Belgium*

# **R-matrix analysis of the total and inelastic scattering cross section of $^{23}\text{Na}$**

**S. Kopecky and A.J.M. Plompen**

## Abstract

*Resonance parameters characterizing the interaction of neutrons with  $^{23}\text{Na}$  in the energy range from 0.3 to 2 MeV were obtained. These parameters describe the total and inelastic cross section. They were obtained from an analysis of data reported by Märten et al. for inelastic and elastic scattering and by D.C. Larson et al. for the total cross section. The data analysis and deduced resonance parameters are presented in some detail. This report serves to clarify the resonance parameters delivered to CEA/Cadarache.*

The inelastic and total cross section data of  $^{23}\text{Na}$  have been analysed in the framework of the R-matrix theory, and the resonance parameters have been determined. Differential elastic cross section data have been used to check the assignment of the orbital angular momentum quantum number of the neutron resonances.

The total cross section data were retrieved from the EXFOR data base, entry number 10761.002. This set of data has been measured by D.C. Larson et al. at ORELA [1]. The elastic and inelastic data have been measured simultaneously by Märten et al. at GELINA. Full details of the experimental setup and the data reduction procedure can be found in refs. [2, 3].

For the measurement 8 2"x2" liquid scintillators were directly coupled to photomultiplier tubes. The detectors were arranged at a distance of 20 cm around the scattering target and their angles, in reference to the beam were: -150, -120, -78, -40, 24, 60, 90 and 136 degrees. The scattering target itself was positioned at 58.5m from the neutron source.

The flux shape was determined with a standard  $^{235}\text{U}$  ionisation chamber which was situated at a distance of 27.5m from the neutron production target. The transmission through the various materials between the uranium sample in the fission chamber and the sample position was calculated. The correctness of the derived flux at the sample position was controlled with measurements of the  $^{10}\text{B}(n,\alpha_1,\gamma)$  cross section and of the carbon differential elastic scattering cross section. Systematic deviations from these standards were found, that within the given statistical uncertainties were the same for both sets of measurements. This was seen as an indication of imperfections on the calculated flux shape at the sample positions. To correct for this deviation an energy dependent correction factor for the neutron flux was determined from these measurements. This additional correction never exceeded 12 %.

For the inelastic cross section the data reduction formula can be given as:

$$\sigma_{\gamma}(E_i) = X_{norm} \frac{\left( \frac{m_i}{D_{m,i}} - \frac{x_b b_i}{D_{b,i}} - b_i^{Al} \right)}{A_i \left( \frac{d\phi}{dt} \right)_i N_{moni} \Delta t n \varepsilon_{\gamma}(E_{\gamma})} - \Delta \sigma_{mult}(E_i)$$

$X_{norm}$  normalization factor determined from the integrated  $^{10}\text{B}(n,\alpha_1,\gamma)$  cross section in the energy range between 0.2-1MeV.

$m_i$  number of y counts in channel i

$D_i$  combined dead-time/multiple shot correction

$b_i$  background in channel i scaled by normalization factor  $x_b$

$b_i^{Al}$  background induced by scattering on sample holder

$A_i$  flux attenuation factor

|                              |  |
|------------------------------|--|
| $d\phi/dt$                   | normalized neutron flux shape distribution as measured with the ionization chamber at 27.5 m, based on the $^{235}\text{U}$ fission standard |
| $N_{\text{moni}}$            | normalization to monitor counts  |
| $\Delta t$                   | time-of flight channel with  |
| $n$                          | sample thickness in atoms/barn   |
| $\varepsilon$                | detection efficiency for the gamma line with energy $E_\gamma$   |
| $\Delta\sigma_{\text{mult}}$ | multiple scattering correction (of order 12-24%)   |

For the inelastic sodium scattering the measured deviation from isotropy were very small, therefore it was possible to derive the total inelastic cross section an integration over the data of the eight detectors.

To deduce the elastic cross section from the registered counts, a dynamic biasing of the detectors as a function of the neutron time-of-flight had to be employed. This approach allowed for a simultaneous measurement of the inelastic and differential cross sections. The main requirement for this approach is an accurate knowledge of the reaction kinematics and the detector efficiency otherwise a bias can be introduced into the data.

The data reduction is done iteratively, at first a provisional differential elastic cross section can be determined by the formula:

$$\sigma_{el}^{prov}(E, \vartheta) = X_{norm} \frac{\left( \frac{n_i}{D_i} - \frac{b_N n_i^{out}}{D_{b,i}} - b_i^\gamma \right)}{n A_i \left( \frac{d\Phi}{dt} \right)_i N_{moni} \Delta t \varepsilon_n(E_1(E, \vartheta))}$$

And with this provisional elastic cross section the final cross section is derived relative to the elastic scattering cross section of carbon as given in an evaluated data file

$$\sigma_{el}^{Na}(E, \vartheta) = \frac{\sigma_{el}^{prov,Na}(E, \vartheta) / C_A^{Na}(E, \vartheta)}{\sigma_{el}^{prov,C}(E, \vartheta) / C_A^C(E, \vartheta)} \left[ \sigma_{el}^{ENDF,C}(E, \vartheta) + \Delta\sigma_{mult}^C(E, \vartheta) \right] - \Delta\sigma_{mult}^{Na}(E, \vartheta)$$

|                 |  |
|-----------------|--|
| $X_{norm}$      | iteratively determined normalization – as it is affected by the multiple scattering corrections  |
| $n_i$           | number of counts in channel i  |
| $D_i, D_{b,i}$  | combined dead-time/multiple shot correction for sample and background respectively   |
| $b_N$           | background scaling factor  |
| $n_i^{out}$     | background spectrum for sample out measurement   |
| $b_i^\gamma$    | $\gamma$ background  |
| $A_i$           | flux attenuation factor  |
| $d\phi/dt$      | normalized neutron flux shape distribution as measured with the ionization chamber at 27.5 m, based on the $^{235}\text{U}$ fission standard   |
| $N_{moni}$      | normalization to monitor counts  |
| $\Delta t$      | time-of flight channel with  |
| $n$             | sample thickness in atoms/barn   |
| $\varepsilon_n$ | detection efficiency for the neutron with energy $E_1$ as a function of the energy of the incoming neutron E and the scattering angle $\theta$ |
| $C_A$           | attenuation correction   |

The normalization constants for inelastic and elastic measurements were agreeing better than 11%. This difference is most likely caused by insufficient knowledge of the detector efficiency.

Before the R-matrix analysis was done, a consistency check of these three data sets was performed. Therefore an integration of the elastic data over  $4\pi$  was performed. In figure 1 the comparison between the total cross section of Larson et al. [3], Cierjacks et al. [4] and the sum (TOT-I) of the elastic data (EL-I) plus the inelastic data (INL) is depicted. The elastic cross section was obtained by direct integration over the angles of the differential cross section data transformed to the centre of mass and to a common energy grid. For the total cross sections, differences starting at approximately 800 keV can be seen, in the region between 1.1 and 1.5 MeV the differences become smaller to increase again above 1.5 MeV. Considering the size of the elastic and inelastic cross sections it is likely that the main difference is due to some errors in the elastic data.

Considering the agreement between the energy dependent normalization factors it can nevertheless be expected that the inelastic cross section should show a similar behaviour. The inelastic data above 1.5 MeV should therefore be considered as potentially biased.

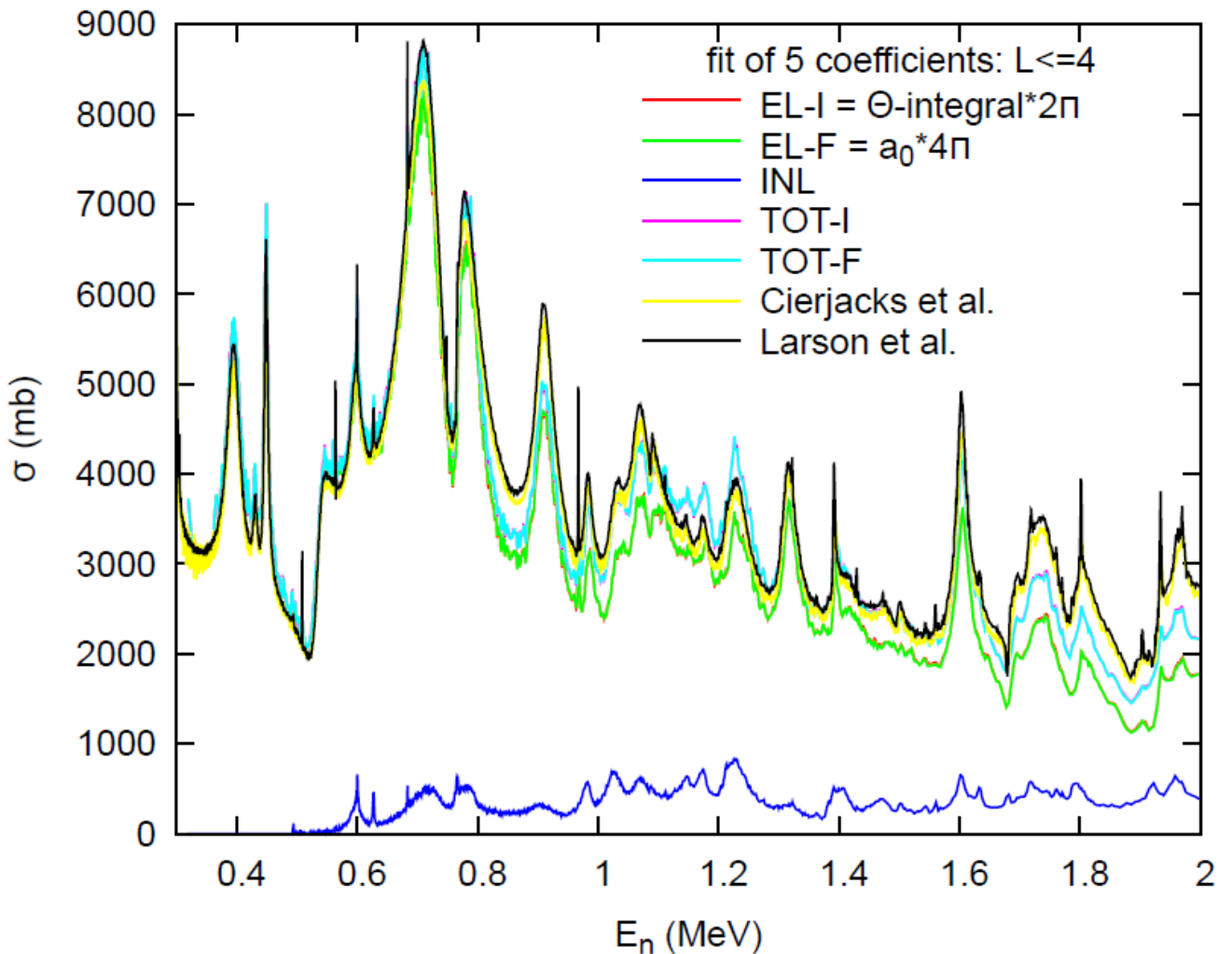


**Fig 1: Comparison between integrated elastic data and inelastic data with total cross section data from the literature**

To check what may be learned from the angular distribution data, Legendre polynomials were fitted into the elastic distribution using the expression

$$\frac{d\sigma}{d\Omega}(\Theta) = \sum_{k=0}^n a_k P_k(\cos\Theta)$$

The value of  $n$  was varied to look for evidence of higher partial wave contributions to the data. The result of the fit for  $n=4$  ( $l \leq 2$ ) is shown in figure 2. These fits showed that only the first three Legendre polynomials are required to describe the data adequately over most of the energy range indicating that in this energy range s- and p-waves dominate. The fourth polynomial (evidence for  $l=2$ ) gives a significant distribution only in the narrow energy regions around 800 keV, 1.2 MeV and above 1.4 MeV. Increasing  $n$  to 8 showed no convincing evidence for  $l=3$  or  $l=4$  contributions. Considering the inconsistencies of the data sets in these energy regions, this contribution could also be due to an error in the differential elastic data. One can therefore conclude that, according to the Blatt-Biederhahn formalism for the differential resonance scattering, not many resonances with an orbital angular momentum quantum number larger than 1 are necessary to describe the observed experimental differential elastic cross section.

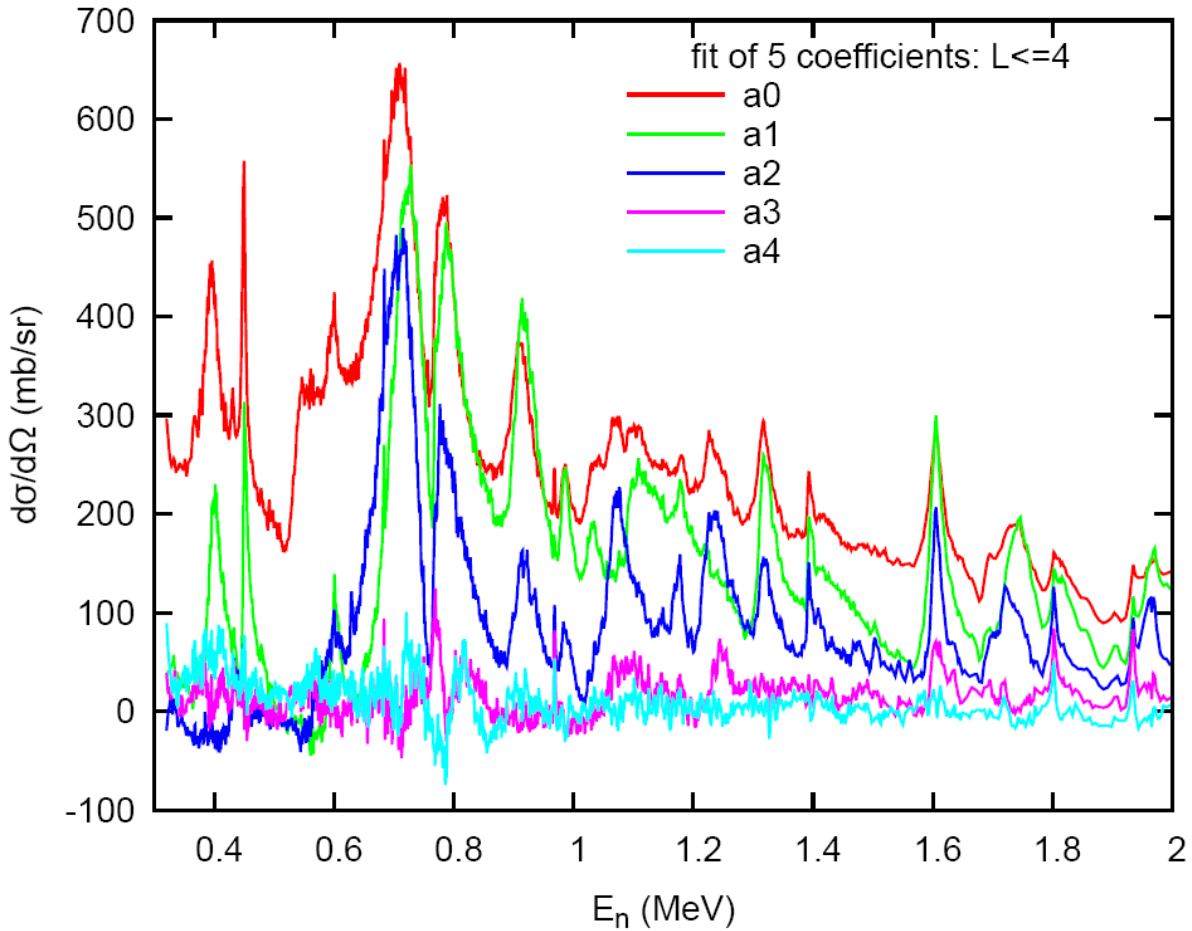


**Fig 2: Coefficients for the Legendre polynomials derived from differential elastic cross section**

The above coefficients may also be used to determine various quantities of interest. One of these, the elastic scattering cross section ( $= 4\pi a_0$ ), is shown in figure 1 as EL-F and corroborates the results obtained by direct integration (EL-I). A similar agreement then follows for the deduced total cross sections (TOT-F and TOT-I). We may now also extract the mean cosine and mean cosine-squared from the data, quantities of interest to transport calculations. This will be done following the discussion of the R-matrix results below.

For the R-Matrix analysis the code SAMMY [5] was employed. This code uses the Reich-Moore approximation to the R-matrix, experimental broadening such as Doppler and resolution broadening

are taken into account. The resolution function in the investigated energy range was approximated by a gauss function. The elastic cross sections were calculated using the Blatt-Biedenharn formalism. Due to the level structure of the Na nucleus – the ground state is  $3/2^+$  and the first excited state is a  $5/2^+$  - for all resonance with  $l > 0$  two elastic and two inelastic channels were used. This approach is different from the original report by Märten et al. But with these additional channels a quite good agreement between experimental data for the inelastic and total cross section could be achieved, see figures 3 and 4. Unlike in the original work broad resonances lying underneath the narrower resonance of the cross sections were not required. The extracted resonance parameters are given in tables 1-4. The elastic differential cross sections were only used to check the orbital angular momentum of the scattered neutrons, i.e. no direct fitting of the experimental data was attempted. In general the assigned J values of the resonances are not unique, i.e. only  $g\Gamma$  was determined. For the analysed energy range a level density parameterization suggests a total number of approximately 120 resonances, of which around 20 should have negative parity and 100 positive parity [6]. The analysis gave 85 resonances of which 35 had negative parity. It can be observed that at forward angles the calculation tends to overestimate the experimental data, whereas at backward angles it tends to underestimate the data (see Fig.5 –Fig. 12) It is not clear if this disagreement is due to the incomplete resonance set, some incorrectly assigned resonance spins or if the experimental data themselves are not fully correct – most likely it will be a combination of all three factors.

As the data sets are inconsistent and the elastic scattering data are considered the main culprit for the observed discrepancies, it might be not surprising that the differences between calculations and experiments are observed. It can be concluded that a new measurements of the angular dependence of the scattering cross section might be called for. The use of an energy dependent normalization factor increases a potential bias in both the elastic and inelastic cross section, and measurements testing the results of these cross sections might be very useful.

To further highlight the differences between the measurements, the elastic cross section, the centre of mass average cosine and cosine-squared obtained from the Legendre fits to the data and obtained from the Sammy-fits are compared in figures 13, 14 and 15. For the cross section differences are evident above 800 keV. Since the R-matrix described the total cross section (Fig. 3) and the inelastic cross section (Fig. 4) the differences between experiment and calculation are similar to those already shown in figure 1 for the total cross section of Larson et al. and those obtained from the present data. For the centre-of-mass average cosine and cosine-squared differences are dramatic over the entire energy range except around 700 keV. Of course in a transport calculation the average cosine in the laboratory is of interest implying a particular combination of the centre-of-mass average cosine and cosine-squared. For reference, the experimental average cosine in the laboratory is given in figure 16 and is shown to lie between 0.15 and 0.4 above 700 keV, while it is markedly lower below this energy. Since this is not very different from the centre-of-mass average cosine it is clear that the R-matrix result will give significantly larger values for this quantity.

## Conclusion

The experimental data of Märten et al.[2] from a simultaneous measurement of the differential elastic scattering cross section and the inelastic scattering cross sections using an array of eight liquid scintillators at the GELINA facility were presented. An R-matrix analysis was made using the code SAMMY [5] including the total cross section data of Larson et al. [1] and the inelastic data of Märten et al. [2]. The parameters are tabulated and the calculated cross sections are compared to the data. Good agreement is obtained for the total and inelastic cross sections. For the differential elastic data differences between data and calculation are often large. It was found that the experimental differential elastic scattering data at best offer qualitative guidance for the resonance analysis, indicating only the more likely value of the orbital angular momentum quantum number.



Integration over angle of the experimental data allows extraction of the elastic scattering cross section and combined with the inelastic cross section this can be compared with the total cross section of Larson et al. and Cierjacks et al. This shows clear differences above 800 keV suggesting energy dependent normalization problems with the differential data. Given the common normalization this may also affect the inelastic data. A Legendre fit to the differential data transformed to the centre of mass allows a confirmation of the elastic scattering cross section obtained by angle integration. It also allows to highlight the large differences in extracted average cosine (and cosine-squared) from the R-matrix calculation and the experimental data. Such large differences affect the diffusion constant in transport calculations in a substantial way.

In order to better understand the deficiencies found between the R-matrix and the differential elastic scattering data and to quantify the impact of the uncertainties for the elastic cross section and the average cosine, new work is needed, both in terms of cross section measurements, their analysis by the R-matrix formalism and their use in transport calculations.

## References:

- [1] D. C. Larson, J.A. Harvey, N.W. Hill, " *Measurement of the total cross section of sodium from 32 keV to 37 MeV*", ORNL-TM-5614, 1976
- [2] H. Märten, J. Wartena and H. Weigmann, " *Simultaneous high resolution measurement of differential elastic and inelastic neutron cross section on selected light nuclei*", GE/R/ND/02/94, 1994
- [3] H. Märten, J. Wartena, H. Weigmann, "  *$\gamma$ -ray production at the threshold of inelastic neutron scattering on light nuclei*", proceedings of the specialists meeting on measurement, calculation and evaluation of photon production data, Nov. 9-11, 1994, ENEA Bologna, Italy
- [4] S. Cierjacks, P. Forti, D Kopsch, L. Kropp, J. Nebe, H. Unseld, " *High resolution total neutron cross sections for Na, Cl, V, Mn and Co between 0.5 and 40 MeV*", KFK-1000, 1969
- [5] N. M. Larson, " *Updated users' guide for Sammy: multilevel R-matrix fits to neutron data using Bayes' equation*", ORNL/TM-9179/R6, 2003
- [6] S. Goriely, S. Hilaire and A.J. Koning, " *Improved microscopic nuclear level densities within the HFB plus combinatorial method*", Phys. Rev. C 78, 064307 (2008).

| Energy [keV] | J   | $\Gamma_\gamma$ [eV] | $\Gamma_n$ [eV] | $\Gamma_{ini}$ [eV] |
|--------------|-----|----------------------|-----------------|---------------------|
| -100.00      | 2.0 | 0.3                  | 2.16E+03        | 0.00E+00            |
| -381.40      | 1.0 | 0.3                  | 2.56E+02        | 0.00E+00            |
| 2.85         | 1.0 | 0.4                  | 3.62E+02        | 0.00E+00            |
| 201.15       | 1.0 | 4.0                  | 7.82E+00        | 0.00E+00            |
| 242.98       | 1.0 | 4.6                  | 4.02E+02        | 0.00E+00            |
| 298.65       | 2.0 | 1.1                  | 2.15E+03        | 0.00E+00            |
| 534.70       | 1.0 | 1.0                  | 3.21E+04        | 3.61E+00            |
| 982.51       | 2.0 | 1.0                  | 1.68E+03        | 7.69E+03            |
| 1118.94      | 1.0 | 2.4                  | 1.92E+05        | 2.38E+02            |
| 1287.23      | 2.0 | 1.0                  | 1.44E+04        | 1.11E+05            |
| 1212.74      | 2.0 | 1.0                  | 5.93E+02        | 8.80E+03            |
| 1392.82      | 1.0 | 1.0                  | 2.95E+05        | 2.00E+04            |
| 1891.90      | 1.0 | 1.0                  | 5.27E+04        | 1.53E+04            |
| 1925.36      | 2.0 | 1.0                  | 6.74E+05        | 3.85E+04            |
| 2142.00      | 1.0 | 3.0                  | 6.99E+04        | 1.00E+03            |
| 3118.00      | 2.0 | 1.0                  | 3.68E+05        | 3.15E+04            |

**Table 1: Parameters of resonances with  $l=0$**

| Energy [keV] | J   | $\Gamma_\gamma$ [eV] | $\Gamma_n$ [eV] | $\Gamma_{ini}$ [eV] |
|--------------|-----|----------------------|-----------------|---------------------|
| 494.50       | 3.0 | 1.0                  | 2.00E+01        | 5.60E+02            |
| 599.89       | 3.0 | 1.0                  | 2.02E+02        | 1.39E+03            |
| 626.72       | 2.0 | 1.0                  | 3.61E+02        | 1.24E+03            |
| 701.65       | 3.0 | 1.0                  | 2.65E+04        | 0.00E+00            |
| 765.48       | 3.0 | 1.0                  | 5.02E+02        | 1.87E+03            |
| 967.35       | 3.0 | 1.0                  | 8.88E+02        | 2.19E+00            |
| 1022.47      | 3.0 | 1.0                  | 4.60E+03        | 3.82E+04            |
| 1064.44      | 3.0 | 1.0                  | 2.62E+04        | 3.58E+03            |
| 1230.72      | 3.0 | 1.0                  | 2.23E+04        | 1.42E+04            |
| 1315.16      | 3.0 | 1.0                  | 2.35E+04        | 2.23E+03            |
| 1392.00      | 4.0 | 1.0                  | 3.64E+03        | 7.83E+02            |
| 1472.26      | 2.0 | 1.0                  | 7.28E+03        | 2.90E+04            |
| 1499.76      | 2.0 | 1.0                  | 2.42E+03        | 8.05E+03            |
| 1588.33      | 3.0 | 1.0                  | 3.40E+01        | 1.95E+03            |
| 1558.66      | 4.0 | 1.0                  | 2.31E+02        | 1.82E+03            |
| 1621.22      | 3.0 | 1.0                  | 1.53E+02        | 4.14E+03            |
| 1737.76      | 3.0 | 1.0                  | 2.04E+04        | 4.51E+04            |
| 1802.91      | 3.0 | 1.0                  | 1.28E+04        | 9.69E+03            |
| 1895.13      | 2.0 | 1.0                  | 4.95E+03        | 3.48E+04            |
| 1928.85      | 3.0 | 1.0                  | 7.53E+03        | 1.64E+04            |
| 2006.58      | 3.0 | 1.0                  | 3.21E+04        | 1.27E+04            |

**Table 2: Parameters of resonances with  $l=2$**

| Energy [keV] | J    | $\Gamma_\gamma$ [eV] | $\Gamma_n$ [eV] | $\Gamma_{inl}$ [eV] |
|--------------|------|----------------------|-----------------|---------------------|
| -0.19        | -1.0 | 0.3                  | 4.71E-01        | 0.00E+00            |
| 35.36        | -2.0 | 0.8                  | 1.09E+00        | 0.00E+00            |
| 53.23        | -2.0 | 1.0                  | 1.01E+03        | 0.00E+00            |
| 117.43       | -1.0 | 1.0                  | 1.87E+01        | 0.00E+00            |
| 213.80       | -0.0 | 4.9                  | 6.54E+03        | 0.00E+00            |
| 236.71       | -1.0 | 1.0                  | 8.56E+01        | 0.00E+00            |
| 239.10       | -2.0 | 1.4                  | 5.74E+03        | 0.00E+00            |
| 299.40       | -1.0 | 1.1                  | 1.25E+02        | 0.00E+00            |
| 305.19       | -0.0 | 1.0                  | 1.31E+01        | 0.00E+00            |
| 430.15       | -0.0 | 1.7                  | 1.69E+03        | 0.00E+00            |
| 508.63       | -3.0 | 1.0                  | 5.87E+01        | 0.00E+00            |
| 563.94       | -1.0 | 1.0                  | 1.11E+02        | 0.00E+00            |
| 596.36       | -2.0 | 1.0                  | 6.58E+02        | 1.24E+04            |
| 683.24       | -2.0 | 1.0                  | 3.18E+02        | 9.68E+01            |
| 711.06       | -3.0 | 1.0                  | 5.90E+04        | 1.05E+04            |
| 748.16       | -0.0 | 1.0                  | 6.19E+02        | 0.00E+00            |
| 775.04       | -1.0 | 1.0                  | 2.58E+04        | 3.08E+03            |
| 780.85       | -3.0 | 1.0                  | 4.64E+04        | 4.42E+03            |
| 896.22       | -1.0 | 1.0                  | 4.36E+04        | 3.90E+03            |
| 908.20       | -2.0 | 1.0                  | 2.76E+04        | 1.06E+03            |
| 978.71       | -1.0 | 1.0                  | 1.33E+04        | 2.20E+03            |
| 1026.64      | -1.0 | 1.0                  | 1.79E+04        | 7.09E+03            |
| 1075.41      | -1.0 | 1.0                  | 2.67E+04        | 5.53E+03            |
| 1091.44      | -1.0 | 1.0                  | 1.85E+05        | 1.51E+03            |
| 1362.12      | -0.0 | 1.0                  | 5.57E+02        | 1.66E+02            |
| 1382.94      | -0.0 | 1.0                  | 3.56E+03        | 4.12E+03            |
| 1404.20      | -2.0 | 1.0                  | 1.13E+04        | 1.22E+04            |
| 1446.44      | -2.0 | 1.0                  | 1.11E+02        | 6.61E+03            |
| 1541.27      | -2.0 | 1.0                  | 7.63E+02        | 5.32E+03            |
| 1593.56      | -2.0 | 1.0                  | 3.53E+04        | 4.94E+03            |
| 1722.64      | -2.0 | 1.0                  | 3.95E+04        | 1.10E+03            |
| 1744.41      | -2.0 | 1.0                  | 1.96E+02        | 2.01E+03            |
| 1786.90      | -2.0 | 1.0                  | 1.73E+03        | 6.03E+03            |
| 1913.33      | -3.0 | 1.0                  | 2.95E+03        | 1.33E+04            |
| 1932.66      | -3.0 | 1.0                  | 5.42E+02        | 1.14E+04            |
| 1957.04      | -3.0 | 1.0                  | 5.05E+04        | 1.19E+04            |
| 2018.00      | -1.0 | 1.0                  | 4.60E+03        | 1.00E+03            |

**Table 3: Parameters of resonances with  $l=1$**

| Energy [keV] | J    | $\Gamma_\gamma$ [eV] | $\Gamma_n$ [eV] | $\Gamma_{inl}$ [eV] |
|--------------|------|----------------------|-----------------|---------------------|
| 597.91       | -1.0 | 1.0                  | 2.57E+04        | 2.58E+03            |
| 1110.93      | -5.0 | 1.0                  | 4.46E+01        | 7.35E+02            |
| 1145.34      | -4.0 | 1.0                  | 3.05E+03        | 2.63E+04            |
| 1172.49      | -4.0 | 1.0                  | 2.34E+03        | 1.17E+04            |
| 1322.48      | -5.0 | 1.0                  | 8.13E+01        | 1.45E+02            |
| 1603.03      | -5.0 | 1.0                  | 1.24E+04        | 2.43E+03            |
| 1631.31      | -3.0 | 1.0                  | 1.71E+03        | 6.11E+03            |
| 1758.98      | -5.0 | 1.0                  | 4.15E+02        | 4.21E+03            |
| 1768.92      | -4.0 | 1.0                  | 4.02E+02        | 5.82E+03            |
| 1899.80      | -5.0 | 1.0                  | 9.35E+01        | 3.57E+02            |
| 1955.25      | -4.0 | 1.0                  | 2.81E+03        | 1.67E+04            |

**Table 4: Parameters of resonances with  $l=3$**

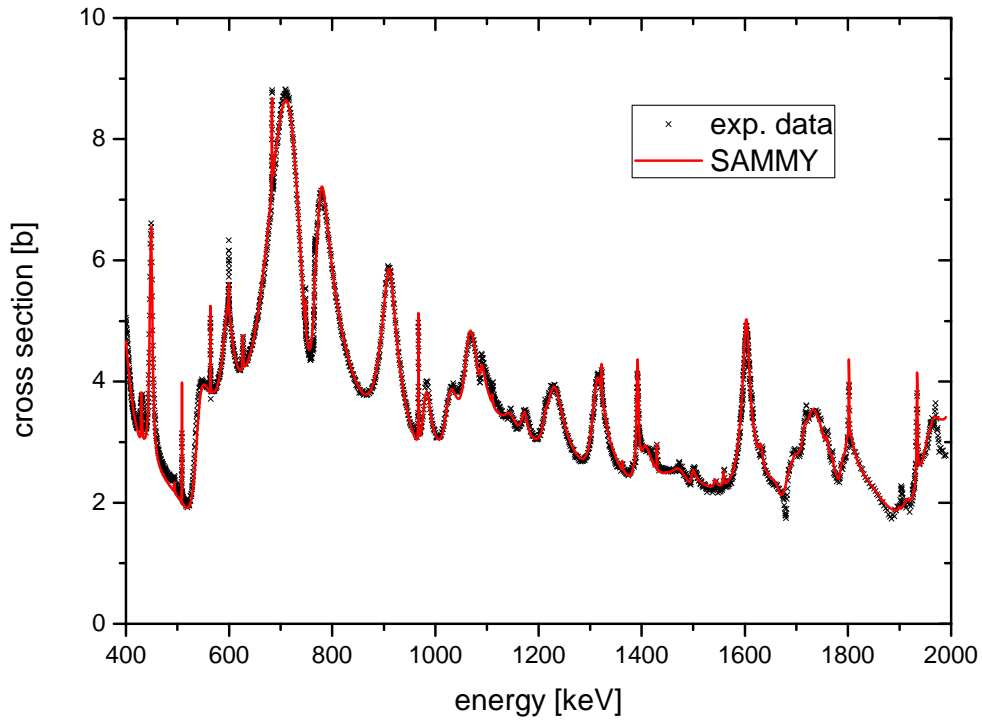


**Fig 3: Comparison of experimental total cross section data of Larson et al. with calculation**

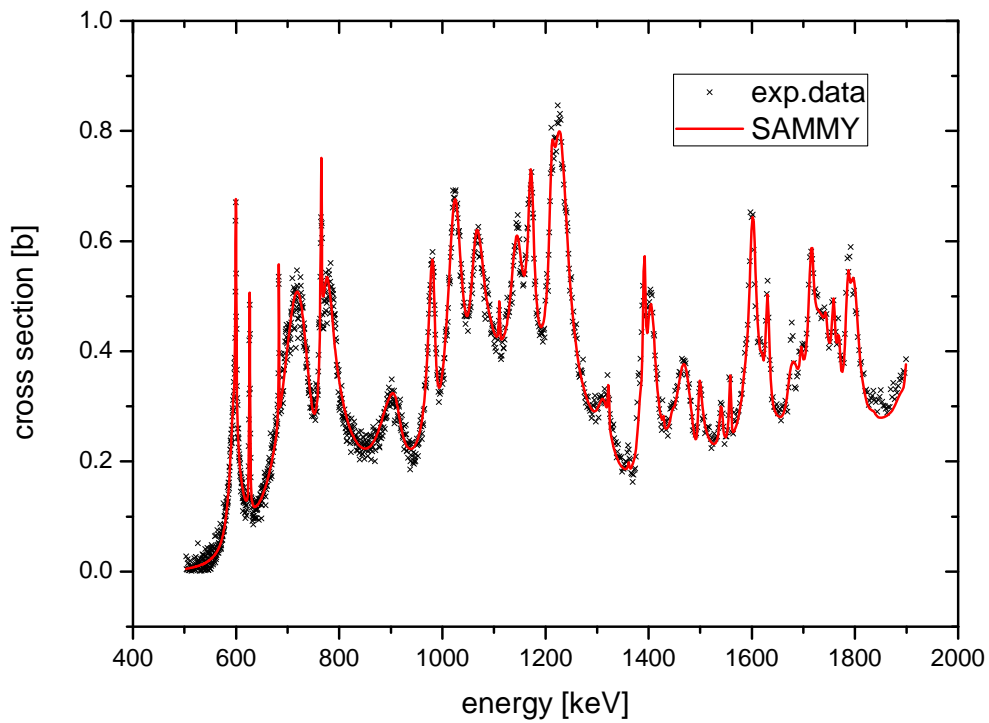


**Fig 4: Comparison of experimental inelastic cross section data with calculation**

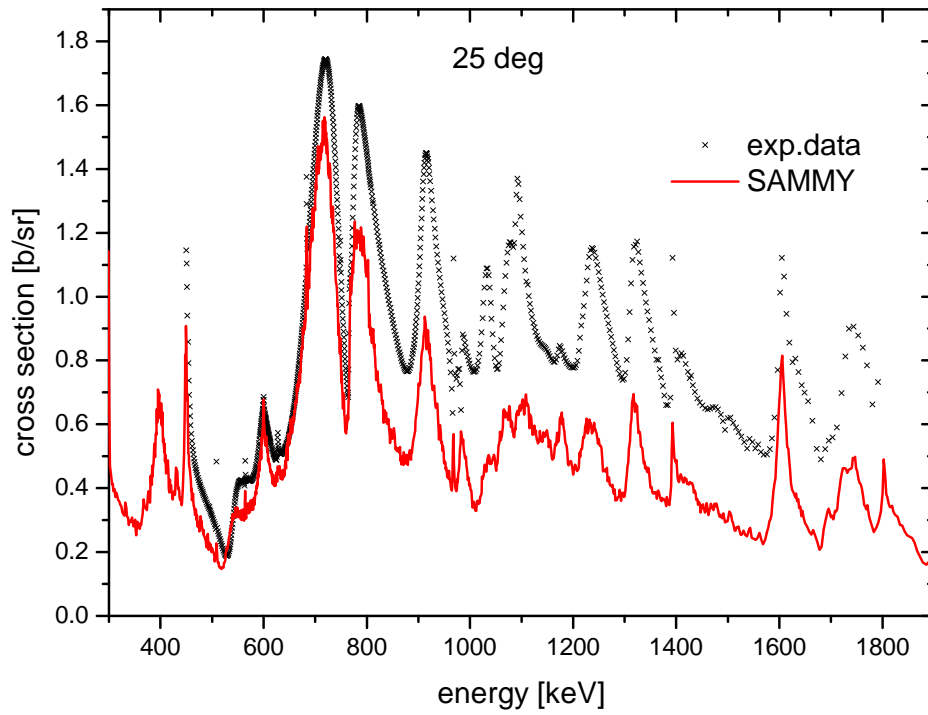


**Fig 5: Comparison of experimental differential elastic cross section data at 25 degrees with calculation**

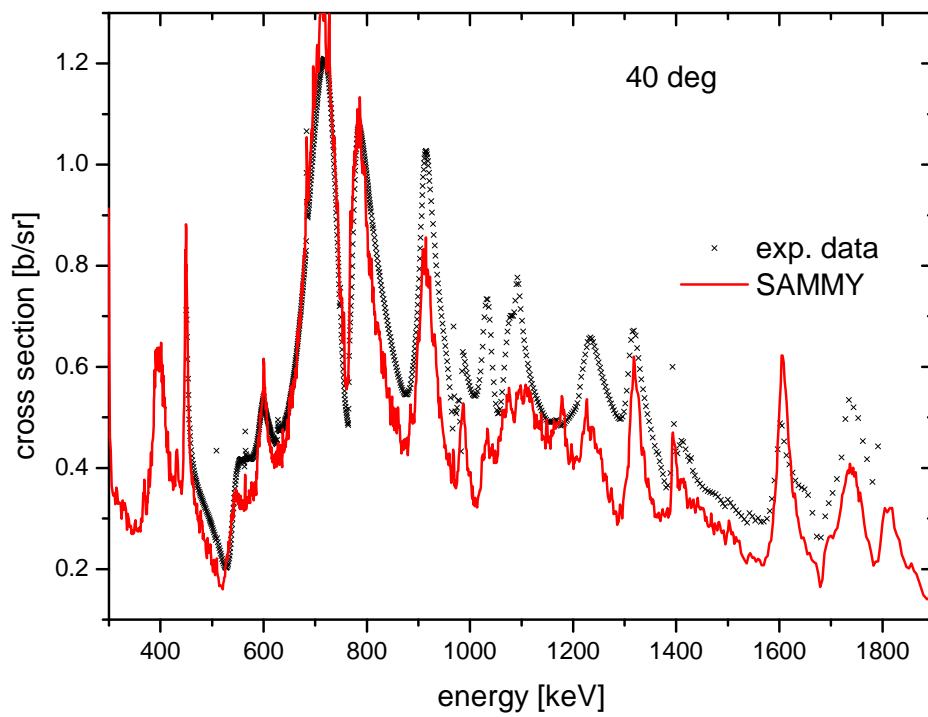


**Fig 6: Comparison of experimental differential elastic cross section data at 40 degrees with calculation**

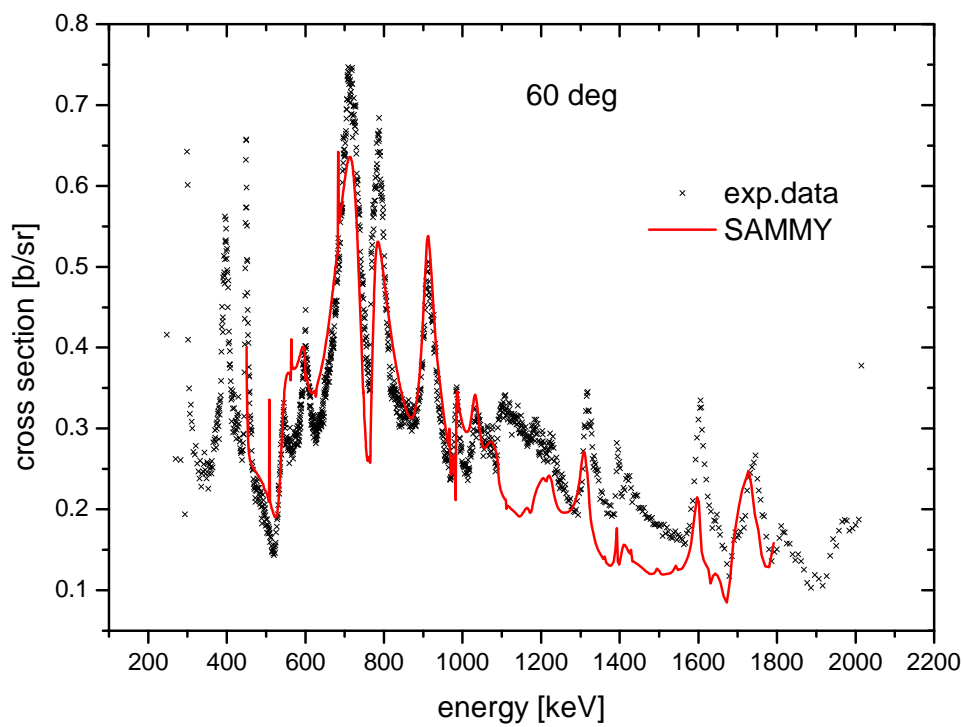


**Fig 7: Comparison of experimental differential elastic cross section data at 60 degrees with calculation**

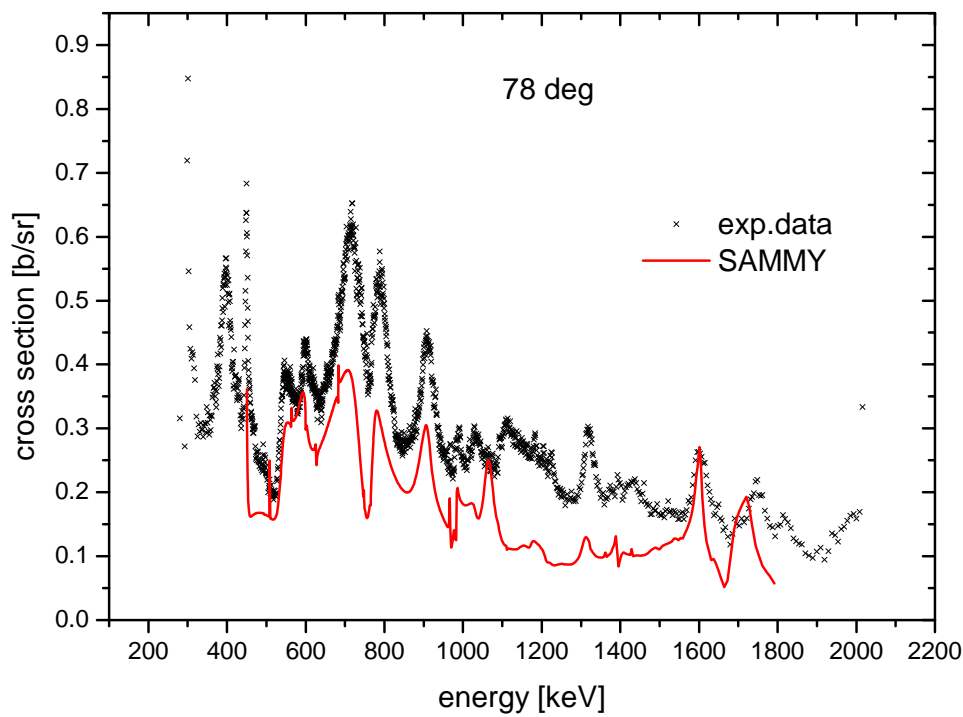


**Fig 8: Comparison of experimental differential elastic cross section data at 78 degrees with calculation**

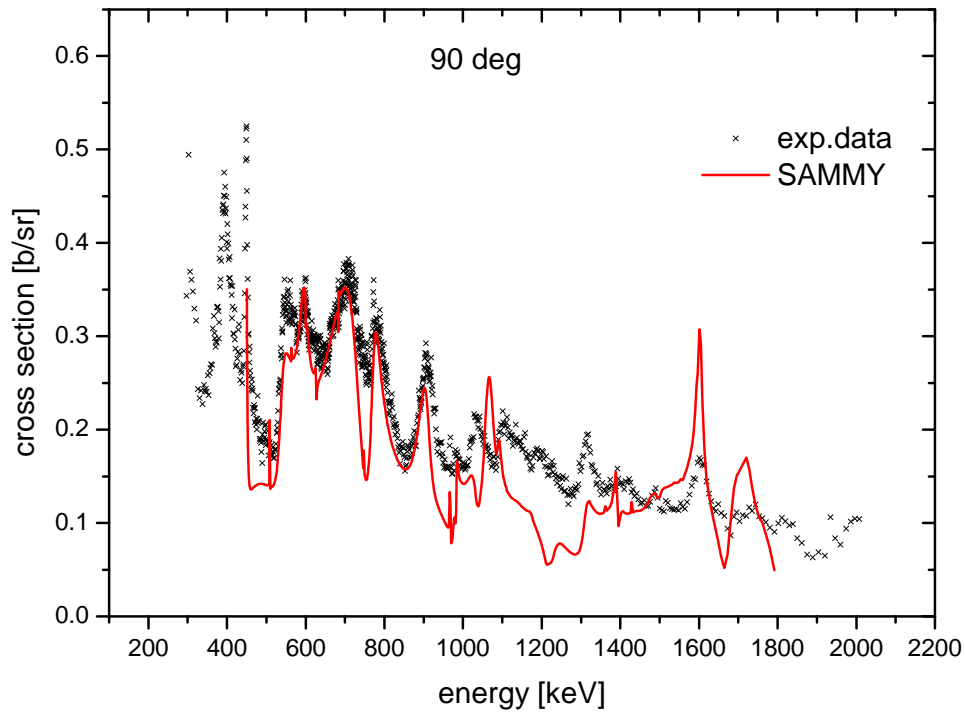


**Fig 9: Comparison of experimental differential elastic cross section data at 90 degrees with calculation**

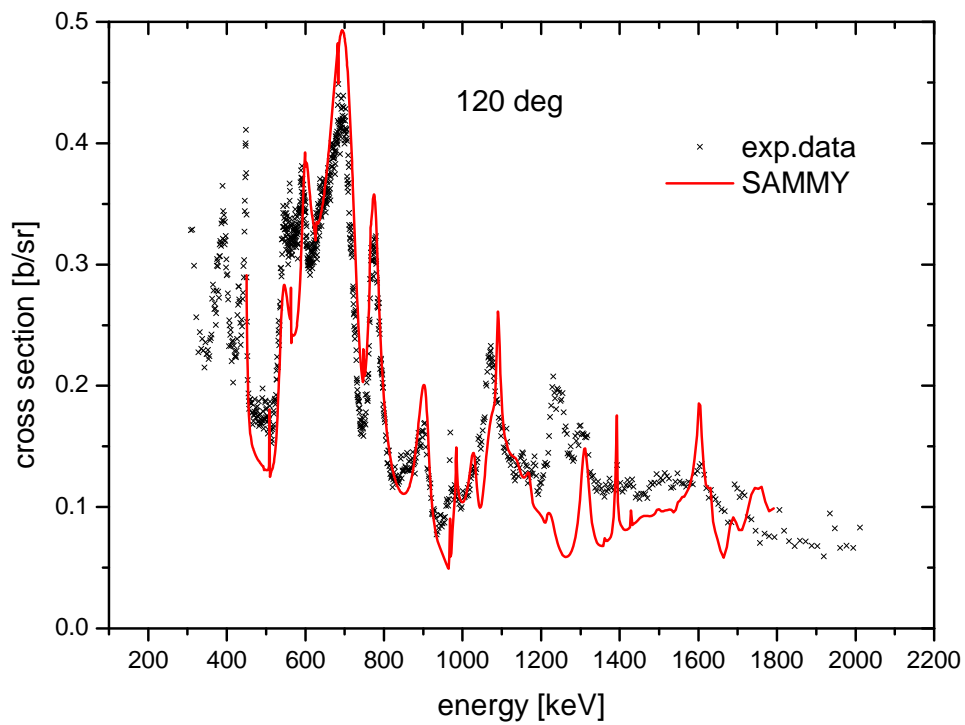


**Fig 10: Comparison of experimental differential elastic cross section data at 120 degrees with calculation**



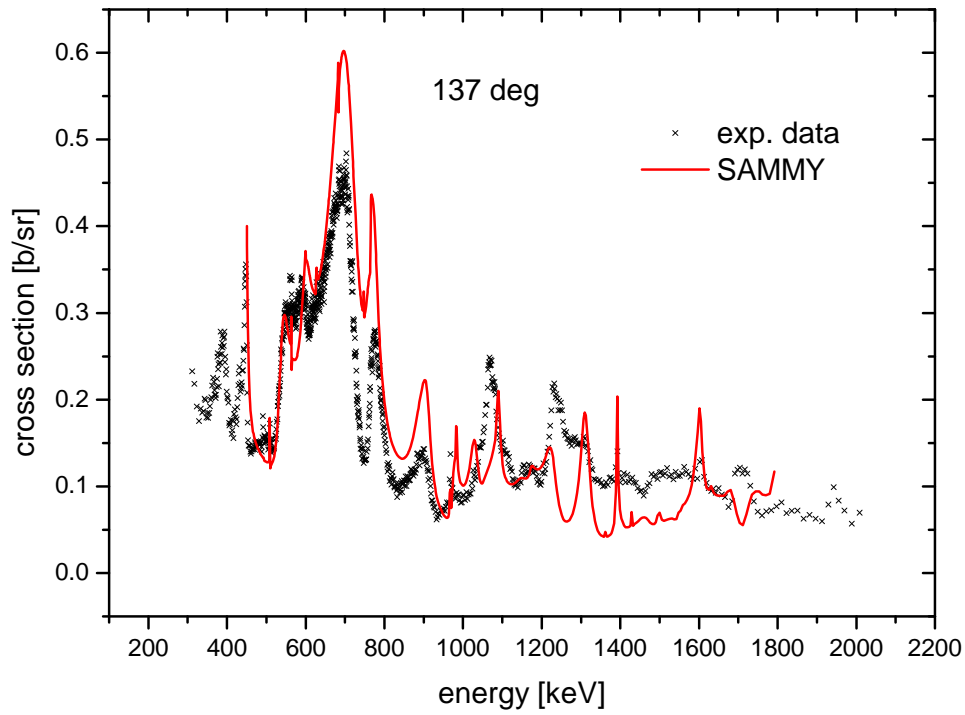


**Fig 11: Comparison of experimental differential elastic cross section data at 137 degrees with calculation**

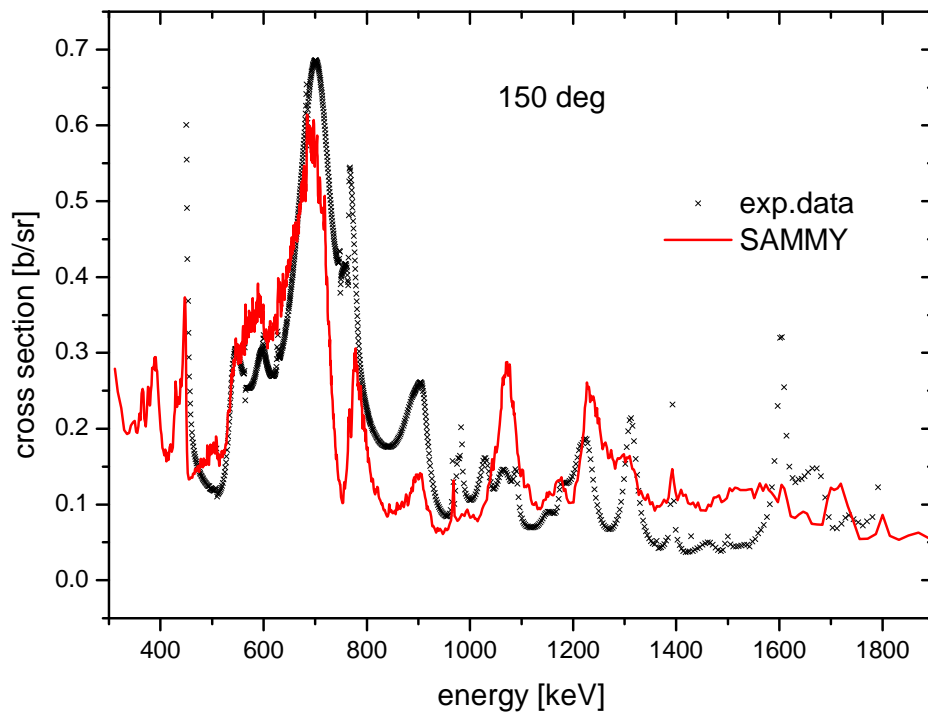


**Fig 12: Comparison of experimental differential elastic cross section data at 150 degrees with calculation**

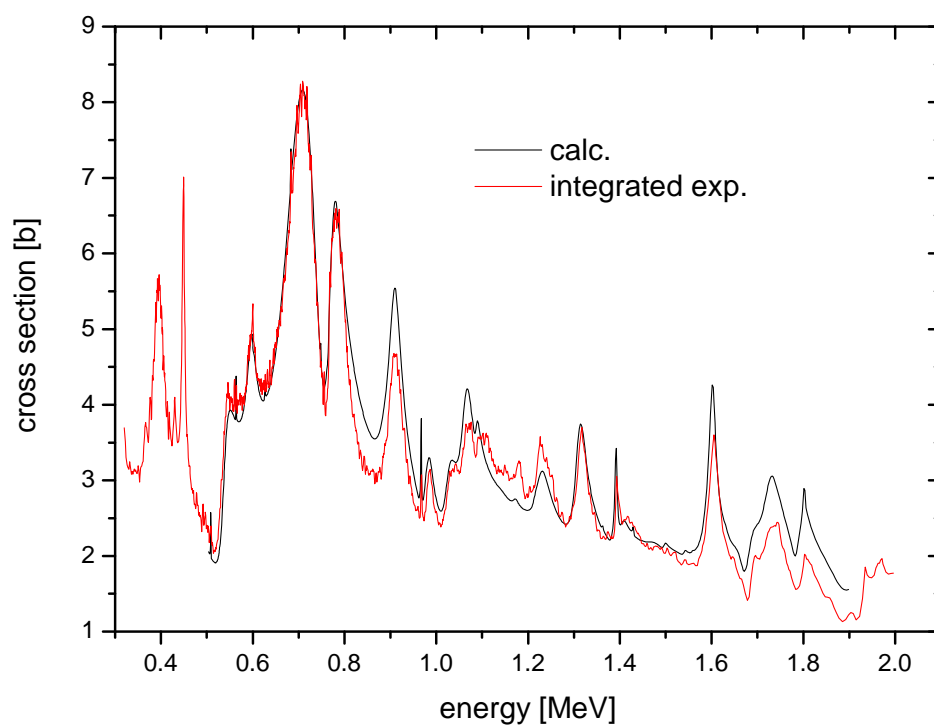


**Fig 13: The elastic scattering cross section from the R-matrix calculation (calc.) and the Legendre fit to the experimental data (Integrated exp.).**

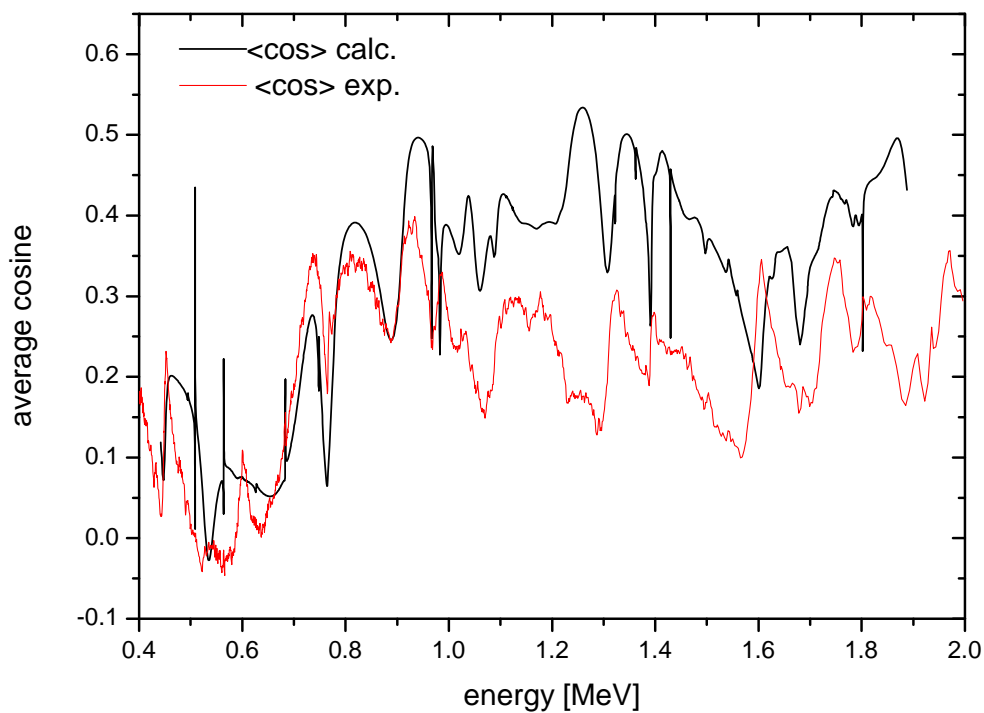


**Fig 14: The centre of mass average cosine from the R-matrix calculation (calc.) and the Legendre fit to the experimental data (exp.).**

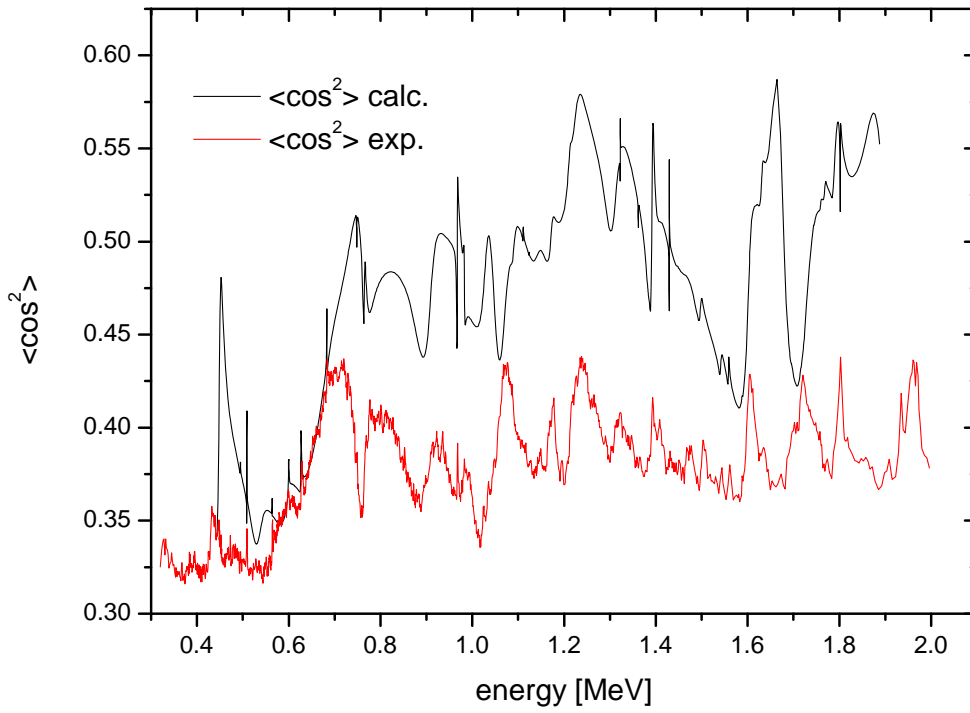


**Fig 15: The centre of mass average cosine-squared from the R-matrix calculation (calc.) and the Legendre fit to the experimental data (exp.).**

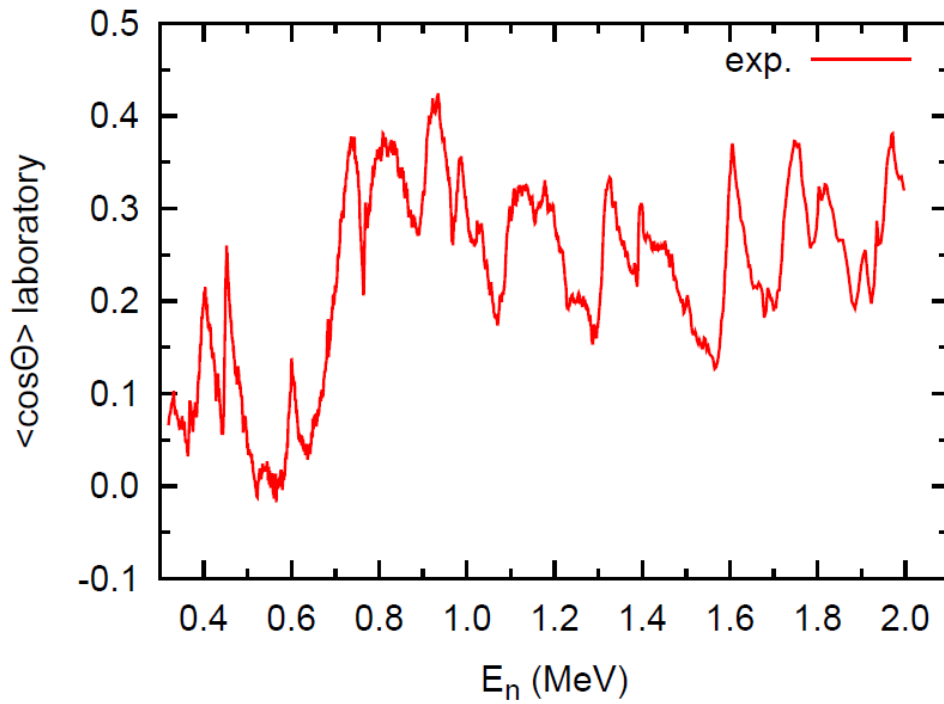


**Fig 16: The laboratory average cosine-squared from the Legendre fit to the experimental data (exp.).**



European Commission

**EUR 25067 EN – Joint Research Centre – Institute for Reference Materials and Measurements**

Title: R-matrix analysis of the total and inelastic scattering cross section of  $^{23}\text{Na}$

Authors: S. Kopecky and A.J.M. Plompen

Luxembourg: Publications Office of the European Union

2011 – 19 pp. – 21.0 x 29.7 cm

EUR – Scientific and Technical Research series – ISSN 1831-9424

ISBN 978-92-79-22214-6

doi:10.2787/55514

**Abstract**

Resonance parameters characterizing the interaction of neutrons with  $^{23}\text{Na}$  in the energy range from 0.3 to 2 MeV were obtained. These parameters describe the total and inelastic cross section. They were obtained from an analysis of data reported by Märten et al. for inelastic and elastic scattering and by D.C. Larson et al. for the total cross section. The data analysis and deduced resonance parameters are presented in some detail. This report serves to clarify the resonance parameters delivered to CEA/Cadarache.

**How to obtain EU publications**

Our priced publications are available from EU Bookshop (<http://bookshop.europa.eu>), where you can place an order with the sales agent of your choice.

The Publications Office has a worldwide network of sales agents. You can obtain their contact details by sending a fax to (352) 29 29-42758.

The mission of the JRC is to provide customer-driven scientific and technical support for the conception, development, implementation and monitoring of EU policies. As a service of the European Commission, the JRC functions as a reference centre of science and technology for the Union. Close to the policy-making process, it serves the common interest of the Member States, while being independent of special interests, whether private or national.

